Detection of small molecules by fluorescence intensity using single dye labeled aptamers and quencher transition metal ions

Blandine Billet, Benoit Chovelon, Emmanuelle Fiore, Patrice Faure, Corinne Ravelet, Eric Peyrin

Detection of Small Molecules by Fluorescence Intensity using Single Dye Labeled Aptamers and Quencher Transition Metal Ions

Blandine Billet,[1,2] Benoit Chovelon,[1,2] Emmanuelle Fiore,[1] Patrice Faure,[1,2] Corinne Ravelet,[1]* and Eric Peyrin[1]*

[1]University Grenoble Alpes, DPM UMR 5063, F-38041 Grenoble; CNRS, DPM UMR 5063, F-38041 Grenoble, France
[2]Biochemistry, Toxicology and Pharmacology Department, Grenoble site Nord CHU – Biology and Pathology Institute, F-38041 Grenoble, France

Corresponding authors:
*eric.peyrin@univ-grenoble-alpes.fr.
*corinne.ravelet@univ-grenoble-alpes.fr.

Abstract

We describe herein an aptamer-based sensing approach that signal the presence of small-molecule targets when fluorescent DNA probes are challenged with the Ni^{2+} or Co^{2+} quencher metal ions. Functional oligonucleotides targeting L-tyrosinamide (L-Tym), adenosine (Ade) or cocaine (Coc) were end-labeled by the Texas-Red fluorophore. A fluorescence quenching occurred upon association of these transition metal ions with the free conjugates. The formation of the target-probe complex, by the way of variations in the overall binding of quencher metal ions along the DNA strands, led to a partial restoration (for the Ade and Coc systems) or a further attenuation (for the L-Tym system) of the fluorescence intensity. The absolute signal gain varied from 40 to 180% depending on the target-probe pair investigated. The approach was also used to detect the compound Ade in a spiked biological matrix in one minute or less. The transition metal ion-based quenching strategy is characterized by its very simple implementation, low cost, and rapid signaling.

Key-words: Fluorescence intensity, aptamers, small targets, quenching, transition metal ions

1. Introduction

Aptamer-based sensors that rely on the fluorescence transduction have been extensively developed over the last twenty years (Fan et al., 2021; Ueno, 2021; Wang et al., 2011). One frequently used approach for the target binding reporting refers to the quenching of a fluorescent dye, conjugated to the aptamer, by an organic molecule (Tan et al., 2016) or a nanomaterial (Liu et al., 2014). The target-induced structural switch of the functional oligonucleotide is converted into a measurable signal change by inhibiting or more commonly restoring the fluorescent response. Despite their wide applications, these methodologies have some limitations. For organic dye-based quenching systems, the presence of two nucleic acid-tethered fluorophores may be particularly prone to side effects on the aptamer recognition properties (Wang et al., 2011). In addition, the synthesis of double-labeled oligonucleotides in aptamer beacons results in a significant cost. Regarding the quenching nanomaterials, one approach is based on the adsorption of fluorescently tagged aptamers to nanostructures, which is often constrained by the slow kinetics of the target-induced desorption of the probe from the surface (Chang et al., 2010) as well as non-specific displacement phenomena (Lopez and Liu, 2021). Another nanomaterial-mediated quenching strategy relies on a capture DNA probe covalently linked to a quenching surface (Kahyaoglu and Rickus, 2018). However, this design requires the careful characterization and control of the surface grafting (Kahyaoglu and Rickus, 2018).

The binding of nucleic acids to metal ions is closely interconnected with the formation of their secondary/tertiary structures and their ability to exert recognition or catalytic functions (Kazakov and Hecht, 2006). Notably, the association of a DNA/RNA receptor with its target molecule can be coupled to changes in affinity and interaction sites for diverse metal ions, as previously exemplified for a variety of nucleic acid-based complexes (Challier et al., 2016; Holmstrom et al., 2014; Kazakov and Hecht, 2006; Keller at al., 2005; Marchand et al., 2015; Mikkelsen et al., 2001; Reuss et al., 2014). This may result from the restriction or exposure of metal ion-binding regions when target-induced structural rearrangements of oligonucleotides occur (Kazakov and Hecht, 2006; Marchand et al., 2015; Mikkelsen et al. 2001). Following this general concept of variations in metal ion binding when the nucleic acid structure/conformation changes, our group has recently reported a novel DNA aptamer-based assay design dedicated to small-molecule sensing (Billet et al., 2021). The binding of certain post-transition/transition metal ions to the aptamer was found to oppose that of its target and concomitantly lead to an improved structural switching process to signal the presence of the analyte. The employed readout technique relied on fluorescence anisotropy (FA) by using an aptamer end-labeled by

the peculiar fluorescein dye as tracer. In the free form, the probe was subjected to neutralization of the backbone negative charges by metal ions. This resulted in improved contacts between the anionic fluorophore and the DNA molecule, which produced an enhancement in the FA ouput through rotational coupling between the two partners. Upon target binding, the repulsion between the attached fluorescein and the backbone was partially recovered due to the release of complexed metal ions, restoring its intrinsic motion and then lowering the signal in an analyte-dependent manner.

Although this assay scheme has proven successful for several target-aptamer systems, a number of limitations may be recognized. Of the metal ions examined, only the Cd^{2+} and Pb^{2+} elements with sufficient potential for perturbing DNA structure were found to be reactive. Indeed, the approach failed to capture modifications in the binding of transition metal ions that display poorer switching activity to DNA (Billet et al., 2021). Furthermore, only fluorophores with a high localized rotational component, *i. e.* negatively charged and with a small ring system, could be effective reporters (Billet et al., 2021). Given these two issues, the assay reveals a definite lack of versatility and a restricted capacity to screen the ion behavior, additionally offering limited possibilities for multiplexed analysis. At this stage, the implementation of alternative transition metal ions that would manifest a novel signaling mechanism toward fluorescent DNA conjugates is therefore highly desirable. Some transition elements are known to exhibit significant fluorescence quenching activities (Kemlo and Shepherd, 1977). These properties have found useful applications in a variety of fields, ranging from the design of metal-dedicated sensors (Mei et al., 2021; Ngororabanga et al., 2019) to the structural analysis of proteins (Yu et al., 2013). For a long time, the quenching features of transition metal ions have only been considered as potential interferences in the development of molecule sensors based on fluorescence signaling aptamers (Rupcich et al., 2006). More recently, the quenching properties as well as the single-stranded DNA binding features of Cr^{3+} have been taken advantage of to design a fluorescent metal ion-based molecular beacon for DNA detection (Ma et al., 2017).

In the present paper, using specifically the Ni^{2+} and Co^{2+} transition metal ions, we introduced a new signaling mode that is based not on the rotational functionality of the reporter but on the quenching of its fluorescence emission. We found that Texas-Red, an electrically neutral fluorophore, is more efficient than fluorescein for detecting target-induced changes in quencher interactions with DNA aptamers. This particular transduction mechanism allowed us to extend the scope of the assay to a broader spectrum of transition metal ions, whose DNA binding and switching capabilities differ appreciably from those of the previously exploited Cd^{2+} and Pb^{2+} species. The general principle is presented in Figure 1. In the target-free state of the probe, the

fluorescence intensity (FI) is attenuated by the DNA-cation interaction that leads to the positioning of quenchers in the vicinity of the dye (Atherton and Beaumont, 1986; Rupcich et al., 2006). Depending on the nature of the different components involved in the reaction, a reduction or an increase in the metal ion binding along the DNA strand could occur upon addition of the target, then triggering a positive or negative change in the FI signal of the reporter, respectively (Figure 1).

In the first stage of this work, we compared the influence of many post-transition/transition metal ions on the fluorescent response of the anti-L-tyrosinamide (L-Tym) DNA aptamer conjugated to two classes of reporters, *i. e.* fluorescein (F) or the Texas-Red (TR). Cu^{2+}, Ni^{2+} and Co^{2+} were shown to be the most efficient quenchers in both cases. We next established that the assay strategy can preferentially operate with the TR conjugate in the presence of Ni^{2+} or Co^{2+}, leading to a further quenching process upon L-Tym addition. The approach was also demonstrated for the adenosine (Ade) and cocaine (Coc) analytes and their corresponding TR-labeled DNA aptamers, implying a reversed phenomenon through a partial restoration of the fluorescence emission signal in the presence of targets. Finally, we showed that the Ade sensor could quickly work under realistic conditions.

2. Experimental section

2.1. Reagents

L-Tyrosinamide (L-Tym), adenosine (Ade), guanosine (Gua), 2-morpholinoethanesulfonic acid (MES), $NiCl_2$, $CoCl_2$, $CdCl_2$, and $MnCl_2$ were purchased from Sigma-Aldrich (Saint-Quentin-Fallavier, France). D-tyrosinamide (D-Tym) was provided from Iris Biotech (Marktredwitz, Germany). Cocaine (Coc) and benzoylecgonine (BZE) were supplied by Lipomed AG (Arlesheim, Switzerland). $CuCl_2$, $HgCl_2$ and $ZnCl_2$ were supplied by ProLabo (Paris, France) and $MgCl_2$ was purchased from Roth (Lauterbourg, France). NaOH was received from Carlo Erba (Val-de-Reuil, France). Free F and TR fluorophores were ordered from Sigma-Aldrich and Acros Organics (Geel, Belgium), respectively. Water was obtained using a Direct-Q® 3UV water purification system (Merck Millipore, Guyancourt, France). The metal ion and analyte stock solutions were prepared in pure water. The MES buffer was prepared to the desired pH by titrating the free acid with sodium hydroxide. Labeled DNA oligonucleotides were synthesized, HPLC-purified and identified by MALDI-TOF mass spectrometry by Eurogentec (Seraing, Belgium). The stock solutions of oligonucleotides were prepared in pure water at 10^{-}

^{3} M and stored at -20°C until use. The DNA oligonucleotides used in the present work are listed in Table S1.

2.2. Measurements

As previously reported (Billet et al., 2021), fluorescence intensity and fluorescence anisotropy were taken on a Tecan Infinite F500 microplate reader (Mannedorf, Switzerland) using black, 96-well Greiner Bio-One microplates (Courtaboeuf, France). Excitation was set at 485 or 585 nm, and emission was collected at 535 or 635 nm for the F and TR fluorophores (free or DNA-conjugated), respectively.

2.3. Metal ion titration of probes

The binding buffer consisted of 50 mM MES, pH 6.3, unless otherwise stated. The working aptamer solutions were obtained by adequate dilution of the stock solution in 10X concentrated binding buffer, with or without target. Prior to the first utilization, the working solutions were heated at 80°C for 5 min and left to stand at room temperature for 30 min in the dark. Successive dilutions of each metal ion stock solution were made in the binding buffer. The aptamer and metal ion working solutions were mixed into the individual wells of a microplate (final volume = 100 µL). All experiments were done at 23°C. Blank wells received 100 µL of the binding buffer. Each well on the first three rows then received 50 µL of the aptamer solution and 50 µL of the metal ion solution. On three other rows, each well received 50 µL of the aptamer solution challenged with 1 mM target (final concentration) and 50 µL of the metal ion solution. The final concentration of the aptamer probe and metal ions was 30 nM and from 0 to 400 µM, respectively. The microplate was then placed into the microplate reader for FI and FA measurements.

2.4. Dose-response curves using TR conjugates

Successive dilutions of L- or D-Tym stock solutions were made in the binding buffer. In a microplate, 50 µL/well of the TR-apt-T or control probe solution containing $NiCl_2$ or $CoCl_2$ at a final concentration of 4 µM and 50 µL/well of the L- or D-Tym solution (final concentration from 0 to 800 µM) were mixed before reading. We carried out similar experiments for Ade or Gua and Coc or BZE (final concentration from 0 to 1 mM) by implementing the TR-apt-A and TR-apt-C (or control) probes, respectively, in the presence of Ni^{2+} and/or Co^{2+}. We used the same binding buffer as metal ion titration experiments.

2.5. Analysis of urine samples and kinetic study

Pooled human urine (batch number: 20BC08) was purchased from ProBioQual (Lyon, France). The urine sample was first centrifuged at 5650 rpm for 10 min. The supernatant was then filtered through 0.45 µm membranes and diluted 20-fold in the 50 mM MES buffer spiked with Ade

(final concentration from 0 to 1 mM). Three replicate samples were analyzed by using 5'-TR-apt-A in the presence of 40 µM Ni^{2+}. The kinetic study was carried out using diluted urine samples. The Ade target (final concentration of 0 or 200 µM) was immediately introduced into the wells containing the probe and 40 µM Ni^{2+}. The reading process was started as quickly as possible (delay time of about 1 min after manual introduction of the microplate into the reader) and measurements were performed through a kinetic run during 15 min, with an interval time of 30s between two successive readings.

3. Results and Discussion

3.1. Selection of quencher metal ions

Some previous works have established that the degree of fluorescence emission quenching for dye-DNA conjugates is highly dependent on the nature of metal ions. As an example, the fluorescent signal of F-labeled oligonucleotides is found to be very strongly inhibited by 100 µM Cu^{2+} whereas other elements such as Zn^{2+}, Mn^{2+}, Hg^{2+} or Cd^{2+} give no or much more limited intensity changes at the same concentration (Li et al., 2017). In addition, using different buffer and F-tagged DNA molecules, Brennan and co-workers have reported that Co^{2+} and Ni^{2+} constitute more efficient quenchers than Mn^{2+} and Cd^{2+} (Rupcich et al., 2006). A variety of dynamic and static mechanisms can be at the origin of the emission quenching by transition metal ions. These notably include ground state complexation, heavy atom effect, electron transfer, Dexter interactions and resonance energy transfer (Birch et al., 1993; Kemlo and Shepherd, 1977; Varnes et al., 1972; Yu et al., 2013), which may be combined in a complex way in the overall phenomenon (Varnes et al., 1972). According to specific mechanistic studies on fluorescent DNA probes (Atherton and Beaumont, 1986; Bregadze et al., 2002; Rupcich et al., 2006), the main processes involved in emission quenching are electron transfer and resonance energy transfer. As such, the reactivity of quencher transition metal ions should arise primarily from their ability to accept electrons from the donor fluorophore and, for colored species acting as potential energy acceptors (including Cu^{2+}, Co^{2+} and Ni^{2+}), from their degree of spectral overlap with the dye.

For selecting quencher cations, the kinetics of the metal ion interaction with DNA should also be considered with great attention. Liu and colleagues have notably shown that the Cr^{3+} quencher displays very slow ligand-exchange rates (Li et al., 2017; Ma et al., 2017), which means that such type of species could not be convenient for our sensing scheme.

In order to choose the most promising quencher metal ions, we initially used as model tracers the 23-mer L-Tym aptamer (apt-T) conjugated, at its 3' extremity, to either F or TR (3'-F-apt-T and 3'-TR-apt-T, Table S1). As compared to F, TR has very distinct chemical and spectral characteristics that may have important implications on its reactivity toward quencher metal ions. First, TR is zwitterionic and contains a large fused ring system, while F is anionic and has a smaller multiple-ring moiety (Unruh et al., 2005a). As the result, TR can engage tighter and larger contacts with neighboring nucleobases (Jahnke et al., 2021; Unruh et al., 2005b), at the extent that it could even be trapped inside the oligonucleotide (Jahnke et al., 2021). So, the two attached dyes are assumed to be dissimilarly surrounded by the DNA moieties, and thus by the metal ions bound to them, so that a different distance-dependent quenching process could occur (Atherton and Beaumont, 1986; Rupcich et al., 2006). Second, the two dyes possess non-identical redox properties (Doose et al., 2009), which have a substantial impact on the electron transfer-based quenching process (Kemlo and Shepherd, 1977). Third, the emission spectrum of the TR dye is shifted to a higher maximum wavelength relative to the F fluorophore (620 nm *vs* 525 nm), resulting in a differential sensitivity toward a potential resonance energy transfer mechanism (Bregadze at al., 2002; Kemlo and Shepherd, 1977; Yu et al., 2013).

The Zn^{2+}, Cd^{2+}, Hg^{2+}, Mn^{2+}, Cu^{2+}, Ni^{2+} and Co^{2+} cations, which potentially cover a large range of quenching activity while displaying a fast ligand-exchange ability, were then brought into contact with probes at 30 nM (Figure 2). The binding buffer (50 mM MES, pH = 6.3) was chosen because of (1) its very low metal ion complexation characteristics and (2) the slightly acidic conditions that are suitable for avoiding metal hydroxide precipitation (Billet et al., 2021). The 3'-TR-apt-T and 3'-F-apt-T probes were shown to undergo small and somewhat irregular FI variations in the presence of 400 µM Zn^{2+}, Cd^{2+}, Hg^{2+} or Mn^{2+}, confirming some previous observations (Billet et al., 2021). A more substantial effect occurred when Cu^{2+}, Ni^{2+} or Co^{2+} were added to the reaction solution. For the F conjugate, it varied from ~40% quenching for Ni^{2+} to ~100 % quenching for Cu^{2+}. The influence of Ni^{2+} on the response of the TR conjugate was more important (FI was divided by about 5), while a less pronounced, but still highly significant, quenching effect was seen for Cu^{2+} (Figure 2). Control experiments with free (unconjugated) fluorescein and Texas-Red fluorophores showed that this quenching process is conditioned by the binding of the metal ions to DNA (Figure S1), in accordance with earlier data (Li et al., 2017; Rupcich et al., 2006).

Considering all these results, we then focused on the Cu^{2+}, Ni^{2+} and Co^{2+} quenchers for investigating their signaling potential in the assay scheme (Figure 1).

3.2. Quencher metal ion-based detection of L-Tym

3.2.1 Responsitivity of 3'-TR-apt-T and 3'F-apt-T probes

Once the quencher metal ions selected, we performed the metal ion titration of the two probes (from 0 to 400 µM), in either their free or target-complexed form (L-Tym at the 1 mM concentration).

As depicted in Figure 3, the addition of increasing amounts of Cu^{2+} resulted in a drastic decrease in the FI signal of both conjugates, not only in the free state (Figure 2) but also in their L-Tym-complexed form. The Cu^{2+} titration curves of 3'-F-apt-T and 3'-TR-apt-T were not significantly affected by the presence of the target. Our previous study has shown that the addition of L-Tym does not alter the ability of soft metal ions such as Hg^{2+} and Ag^{+} to interact with apt-T (Billet et al., 2021). The preferential binding of these cations to nucleobases (Hackl et al., 2005; Sissoeff et al., 1976) determines the dramatic disruption of the active structure of DNA (Zhou et al., 2010), which defeats the L-Tym-oligonucleotide association. Cu^{2+} has a binding preference for bases close to those of Hg^{2+} and Ag^{+} metal ions (Hackl et al., 2005) and thereby can also cause severe disorganization in DNA structures (Eichhorn et al., 1968). Hence, the L-Tym-bound form of the aptamer probes might be also completely disadvantaged by the interaction of Cu^{2+} with DNA.

Compared to Cu^{2+}, Ni^{2+} and Co^{2+} exhibits a much lower nucleobase-to-phosphate binding affinity ratio, which approximates that of hard metal ions more than that of soft metal ions (Eichhorn et al., 1968; Hackl et al., 2005; Sissoeff et al., 1976). As such, their impact on nucleic acid architectures is generally more weighted and balanced (Sissoeff et al., 1976), fluctuating between stabilizing (Eichhorn et al., 1968; Sorokin et al., 2001) and destabilizing (Sorokin et al., 2001) effects related in part to the nature and structure of the DNA. It is thus unlikely that these metal ions would induce total neutralization of the target-aptamer association. We recorded Ni^{2+} and Co^{2+} titration curves that differ as a function of the probes. For the F conjugate, we did not clearly achieve saturation of the fluorescence quenching process in the concentration range of the metal ions, in the absence or presence of the target (Figure 3). The FI variations appear to be in concert with an only slight change in the titration curves upon addition of L-Tym, revealing that the metal ion binding capacities of the free and target-bound states of 3'-F-apt-T are poorly differentiable over the range tested. In contrast, the quenching due to Ni^{2+} and Co^{2+} reached saturation for both free and target-bound 3'-TR-apt-T, and was paralleled by a noticeable shift of the metal ion titration curves to the left in the presence of L-Tym (Figure 3). This suggests that the association between the target and the TR-labeled aptamer is coupled to an enhanced stability of binding between metal ions and DNA. The observation is similar to what is often retrieved for functional nucleic acids when they are

challenged with conventional stabilizing cations such as the Mg^{2+} hard metal ion (Challier et al., 2016; Holmstrom et al., 2014; Reuss et al., 2014).

Given the distinct L-Tym-dependent response of 3'-F-apt-T and 3'-TR-apt-T in the presence of Ni^{2+} and Co^{2+}, it is apparent that, beyond its role in the extent of quenching, the nature of the dye has a crucial weight on the target signaling ability of the probe (see also below for the two other investigated systems). As discussed above, TR can share a wider area of contacts with the DNA chain than F (Jahnke et al., 2021; Unruh et al., 2005b), which would make the reporter capable of more intimately probing target-induced perturbations in the binding of quenchers to DNA sites. Moreover, these findings are in accordance with other data collected for fluorescently labeled proteins, which respond to target-mediated conformational changes in different ways depending on the type of grafted fluorophores that are faced with quencher transition metal ions bound to nearby regions (Yu et al., 2013).

To further appreciate the potential of the quenching-based assay scheme presented here, we analyzed the data through exactly the same readout approach implemented in our previous work, namely the FA technique (Billet et al., 2021). On one hand, we recorded a significant enhancement in the FA output with the target-free 3'-TR-apt-T upon addition of $Co^{2+}$and Ni^{2+}, the FA variation spanning the 0.060-0.100 range (Figure S2). The FA gain can be closely correlated with the degree of fluorescence quenching (Figure S2). This supports that the fluorescence lifetime shortening, which is well known to occur when dye emission is quenched by Ni^{2+} and Co^{2+} metal ions (Atherton and Beaumont, 1986; Rupcich et al., 2006), is most directly involved in the anisotropy increase (Zhang et al., 2012). Such event was concomitant with a substantial target-dependent FA response of 3'-TR-apt-T for the two quenchers (Figure S2). On the other hand, 3'-F-apt-T responded more weakly to the addition of metal ions, as illustrated by the FA increase ranging from only 0.010 (Co^{2+}) to 0.040 (Ni^{2+}) (Figure S2). The small change in anisotropy for Ni^{2+} appears to come straight from its rather modest quenching effect on the F emission while the very limited FA variation seen with Co^{2+} suggests the involvement of a proper depolarization process (Figures 3 and S2). In any case, 3'-F-apt-T exhibited no differential behavior in the absence or presence of L-Tym (Figure S2). All data emphasize that the TR conjugate also responds in FA more sensitively not only to the binding of the quencher metal ion but also to its fluctuations depending on the formation of the L-Tym-apt-T complex.

3.2.2. Effects of the label position and aptamer length on the probe responsivity

We next assessed the influence of the terminal position of the fluorophores on the reactivity of the probes using the representative Ni^{2+} quencher. The 5’ end TR and F conjugates of apt-T (5'-

TR-apt-T and 5'-F-apt-T, Table S1) showed FI changes upon quencher binding as well as L-Tym dependent responses close to those reported with the corresponding 3'-end conjugates (Figure S3 *vs* Figure 3). The results indicate that the terminal location of the reporter does not significantly alter the responsivity features of the apt-T probe.

In contrast, the use of a longer version of apt-T, *i. e.* one aptamer sequence bearing an additional 15-mer strand at the 5' end (Challier et al., 2016) (5'-TR-apt-T-L, Table S1), resulted in the complete loss of the L-Tym-dependent titration curve shift (Figure S3). The supplementary region could act by altering the overall shape of the aptamer or, if it is rather inert toward it, by shielding changes in the Ni^{2+} binding to the 23-mer motif.

3.2.3. Dose-response curves using TR conjugates

Considering the favorable curve shift obtained with 3'-TR-apt-T, we then decided to titrate this TR-labeled aptamer with increasing amounts of L-Tym, in the presence of 4 µM Ni^{2+} or Co^{2+} (Figure 4). For comparison, the dose-response curve in the absence of these metal ions is also depicted in Figure S4. In such a case, only a small FI increase (less than 8 %) was measured upon exposure of 800 µM L-Tym. As expected from the metal ion titration curves (Figure 3), the probe operated through further fluorescence quenching (~40-50%) upon addition of target. The assay specificity was assessed by testing the non-cognate D-Tym enantiomer as well as a non-binding DNA probe of similar length (5'-TR-apt-A, Table S1). The FI signal was roughly invariant over the analyte concentration range, demonstrating that the fluorescent response of the 3'-TR-apt-T sensor is related to the target-aptamer recognition process.

We next investigated the influence of adding metal ions typically used in the aptamer binding solutions, *i. e.* the alkali Na^+ and alkaline earth Mg^{2+}, on the 3'-TR-apt-T response. Ni^{2+} at 4 µM was used as quencher. For the analysis of the Na^+ effects, the MES buffer was varied from 50 to 500 mM, corresponding to a change in [Na^+] from ~30 to ~300 mM. For its part, Mg^{2+} was introduced into the 50 mM MES buffer at a concentration up to 5 mM. As shown in Figure S5, a significant decrease in signal gain was reported with these two species at their highest concentration. The impact of these added cations on the ionic atmosphere of the DNA is thought to determine a reduced association of the quencher ion with apt-T (Draper, 2004) and thus a deterioration of the signaling process. The significant effect observed even at a low amount of Mg^{2+} could denote a specific competition of this divalent cation with Ni^{2+} for its DNA binding sites (Kazakov and Hecht, 2006).

When challenged with Ni^{2+} or Co^{2+}, the binding of 3'-TR-apt-T to L-Tym leads to an apparent K_d in the 0.13-0.34 µM range (Table S2). As a point of comparison, the dissociation constant of the complex between L-Tym and unmodified apt-T is around 10 µM under Mg^{2+}-free

reaction conditions (Challier et al., 2016). This reveals that the simple addition of Ni^{2+}/Co^{2+} to the reaction solution at a low micromolar concentration results in a highly stabilized target binding state. As the result, the detection limit (determined from a signal-to-noise ratio > 3) for L-Tym was 10 nM in the presence of the Ni^{2+} quencher, the lowest ever reported for homogeneous-phase aptasensors without signal amplification (Billet et al., 2021). It was associated to a linear range extending to 250 nM (Figure S6).

Finally, we also performed dose-response experiments by using the 5'-end TR conjugate in the presence of 4 µM Ni^{2+}. We found that the overall signal variation is roughly equivalent to that reported with 3'-TR-apt-T under the same conditions, demonstrating that the terminal location of TR has a minimal effect on sensor efficiency and apparent affinity of L-Tym for apt-T (Table S2).

3.3. Quencher metal ion-based detection of Ade

In order to explore the generalizability of the sensing approach, we next tested our method on another target-aptamer pair. We focused on the very widely studied anti-adenosine (Ade) 25-mer DNA aptamer (apt-A) that exhibits a different binding motif relative to apt-T (hairpin-like for apt-A (Durand et al., 2014) *vs* no stable structure for apt-T (Challier et al., 2016)).

The F/TR conjugates at the 5' end (5'-F-apt-A/5'-TR-apt-A, Table S1) and the Ni^{2+}/Co^{2+} ions were initially used as probes and quenchers, respectively. The metal ion titration curves of the two probes were constructed in the absence or presence of Ade (1 mM, Figure 5). Similarly to what was observed for the L-Tym system, the metal ion-dependent FI signal of the F conjugate was approximately insensitive to the presence of target. In contrast, we noticed a substantial rightward shift in the titration curves of the TR conjugate upon exposure of Ade. The result agrees with a reduced ability of 5'-TR-apt-A to associate with these metal ions in its bound form. This follows the trend encountered for various aptamers facing stronger base binders, *i. e.* the softer Cd^{2+} or Pb^{2+} species (Hackl et al., 2005; Sissoeff et al., 1976), where the target-bound DNA state opposes that complexed to metal ions (Billet et al., 2021).

In accordance with the results from the L-Tym system, the TR conjugate was found to be more conducive than the 5'-F-apt-A tracer to sense the formation of the Ade-apt-A complex through FA readout (Figure S7). Furthermore, using the aptamer carrying the labels at the other extremity (3'-TR-apt-A and 3'-F-apt-A, Table S1) in the presence of Ni^{2+} gave a trend in FI similar to that of the 5'-end conjugates (Figure S8), although the Ade-dependent response obtained with 3'-TR-apt-A was not as pronounced as that of 5'-TR-apt-A (Figure 5).

The reactivity of the Ade-apt-A complex toward Ni^{2+}/Co^{2+} ions is shown to be reversed relative to that observed with the L-Tym-apt-T complex. Given that these metal ions react with

phosphates and nucleobases in a somewhat balanced way (see above), we could propose that one of these contributions predominates over the other on a case by case basis, depending on the binding sequence and target-induced conformational rearrangements (large for apt-T (Challier et al., 2016) *vs* moderate for apt-A (Xia et al., 2013)) of the aptamers.

The dose-response curves for Ade using 5'-TR-apt-A, recorded by using a medium containing 40 µM Ni^{2+} or 400 µM Co^{2+}, are depicted in Figure 6. Of note, no significant FI change was reported upon addition of Ade in the absence of transition metal ions (Figure S4). In accordance with the metal ion titration data observed with or without Ade, the curve exhibited a partial restoration of the fluorescence intensity upon exposure of increasing amounts of the target. The fluorescence signal was enhanced by ~180% at 1 mM target in the presence of 40 µM Ni^{2+} while a lower but still exploitable FI increase (~60%) was measured with 400 µM Co^{2+}. The assay response was also shown to be Ade binding-specific as the non-cognate guanosine (Gua) analyte and a control probe (3'-TR-apt-T) provided no significant FI variations in the presence of the two quenchers.

Because of the counteracting probe-binding effects of Ade and Ni^{2+}/Co^{2+} ions (Billet et al., 2021), the affinity of 5'-TR-apt-A for the target was rather reduced in the presence of quencher cations. Indeed, we determined an apparent K_d varying from 105 to 155 µM (Table S2) while the dissociation constant of the native complex is around 10 µM in Mg^{2+}-free conditions (Gulbakan et al., 2018). Consequently, a somewhat high detection limit was found (8 µM by using the Ni^{2+} quencher). However, the value satisfactorily compares with those estimated from a number of quencher-based fluorescent aptamer assays for Ade and related targets (Kahyaoglu and Rickus, 2018; Lopez and Liu, 2021; Nutiu and Li, 2003). As shown in Figure S6, the linear range of the assay was 0-200 µM.

Here again, further dose-response experiments were carried out using the 3'-TR-apt-A tracer in the presence of 40 µM Ni^{2+}. Although a smaller signal gain was realized compared to 5'-TR-apt-A (55% *vs* 180% increase in FI), the sensor nevertheless operates with an identical apparent affinity between Ade and apt-A (Table S2).

3.4. Quencher metal ion-based detection of Coc

To further consider the generic potential of the strategy, we finally decided to concentrate on the anti-cocaine (Coc) 30-mer DNA aptamer (apt-C) that displays another type of binding motif, *i. e.* a three-way junction structure (Billet et al., 2021). In this context, we implemented four TR/F conjugates (5'-TR-apt-C, 5'-F-apt-C, 3'-TR-apt-C and 3'-F-apt-C, Table S1) and the Ni^{2+} quencher ion. All the experimental results are depicted in Figures S6, S9, S10 and Table S2. To briefly summarize, we observed that (1) the TR conjugates can specifically respond to the target

with a better signal gain than the F probes (Figure S9) and (2) the signaling behavior resembles that of the Ade system, but with a lesser signal gain (approximately 60%) upon target binding (Figure S10 and Table S2).

3.5. Potentialities for complex sample analysis

We assessed the capability of our sensor to work under real-life conditions. We chose the Ade-5'-TR-apt-A pair and a biological fluid as study model. A 5% human urine sample was spiked with the Ade analyte at different concentrations, in the presence of 40 µM Ni^{2+}. The Ade dose-response curve was then constructed as depicted in Figure S11. The normalized response was shown to be comparable to that recorded in buffered solution, suggesting that the sensor could retain its activity in diluted complex matrices.

The time-dependent FI output of 5'-TR-apt-A upon addition of 200 µM Ade to the urine sample was also recorded. We found that the reaction equilibrium can be reached in a short period of time, *i. e.* within one minute or less (Figure S11). This data demonstrates that the aptasensor is able to promptly respond to the presence of the target, even in a realistic medium.

4. Conclusion

In summary, we have demonstrated that Ni^{2+} and Co^{2+} transition metal ions can be used as fluorescence quenchers for designing sensors through their differential sensitivity to the free *vs* bound state of TR-conjugated aptamers. Unlike the previously deployed Cd^{2+} and Pb^{2+} elements (Billet et al., 2021), Ni^{2+} and Co^{2+} appear to be particularly suitable, given their position in the classification of base-to-phosphate binders (Hackl et al., 2005), for either favoring or opposing the formation of target-aptamer complexes. In this regard, we have found with interest that these two metal ions, which are not generally used for this purpose in the aptamer field, greatly stabilize the target-bound state of the TR-apt-T probes, leading to a very strong improvement in the binding affinity (by a factor of about 100 in the presence of Ni^{2+}). This point emphasizes that certain transition elements, preferentially those with not too strong affinity for nucleobases, could be an alternative to the usual alkaline earth ions such as Mg^{2+} or Ca^{2+} for stabilizing some peculiar active aptamer structures (Keller et al., 2005; Zimmermann et al., 2000).

Small-molecule binding aptamers, labeled with a single dye at one extremity, most often generate limited FI responses under the direct signaling configuration due to small target-induced alterations in the terminal DNA regions (Jhaveri et al., 2000; Merino and Weeks, 2005; Stojanovic et al., 2001; Zhao et al., 2014). The addition of quencher transition metal ions to the binding solution provides a useful route to promote signal output for aptamer probes that display no or minimal responsivity, as exemplified in Figures S4 and S10. Furthermore, despite the fact

that the use of these transition metal ions requires some precautions in terms of handling and waste management, the current design provides a simpler and/or less expensive method compared to the most commonly used quenching strategies in aptasensor development. Although the implementation of the TR reporter through the current design is particularly advantageous for detecting target-induced changes in aptamer-bound quenchers, the absolute signal gain achieved for the three systems studied here remains still moderate (ranging from 40 to 180%). Future works will therefore focus on screening a wider range of fluorophores to select better reporter/quencher ion combinations.

Funding

We acknowledge the support of NeuroCoG (ANR-15-IDEX-02), Labex Arcane and CBH-EUR-GS (ANR-17-EURE-0003), and Polynat Carnot Institute (ANR-11-CARN-007-01).

CRediT authorship contribution statement

Blandine Billet: Methodology, Validation, Data curation, Investigation, Writing – original draft. Benoit Chovelon: Supervision, Data curation, Investigation, Writing – original draft. Emmanuelle Fiore: Methodology, Investigation. Patrice Faure: Supervision, Writing – review & editing. Corinne Ravelet: Funding acquisition, Supervision, Writing – review & editing. Eric Peyrin: Conceptualization, Project administration, Supervision, Funding acquisition, Writing – review & editing.

References

Atherton, S. J., Beaumont, P. C. J. Phys. Chem. 1986, 90, 2252-2259.
Billet, B., Chovelon, B., Fiore, E., Oukacine, F., Petrillo, M-A., Faure, P., Ravelet, C., Peyrin, E. Angew. Chem. Int. Ed. 2021, 60, 12346–12350.
Birch, D. J. S., Suhling, K., Holmes, A. S., Salthammer, T., Imhof, R. E. Pure Appl. Chem. 1993, 65, 1687-1692.
Bregadze, V., Khutsishvili, I., Chkhaberidze, J., Sologhashvili, K. Inorg. Chim. Acta 2002, 339, 145-159.
Challier, L., Miranda-Castro, R., Barbe, B., Fave, C., Limoges, B., Peyrin, E., Ravelet, C., Fiore, E., Labbé, P., Coche-Guérente, L., Ennifar, E., Bec, G., Dumas, P., Mavré, F., Noël, V. Anal. Chem. 2016, 88, 11963-11971.
Chang, H., Tang, L., Wang, Y., Jiang, J., Li, J. Anal. Chem. 2010, 82, 2341-2346.
Doose, S., Neuweiler, H., Sauer, M. ChemPhysChem 2009, 10, 1389-1398.
Draper, D. E. RNA 2004, 10, 335-343.
Durand, G., Lisi, S., Ravelet, C., Dausse, E., Peyrin, E., Toulmé, J. J. Angew. Chem. Int. Ed. 2014, 53, 6942-6945.
Eichhorn, G. L., Shin, Y. A. J. Am. Chem. Soc. 1968, 90, 7323-7328.

Gulbakan, D., Barylyuk, K., Schneider, P., Pillong, M., Schneider, G., Zenobi, R. J. Am. Chem. Soc. 2018, 140, 7486−7497.
Hackl, E. V., Kornilova, S. V., Blagoi, Y. P. Int. J. Biol. Macromol. 2005, 35, 175–191.
Holmstrom, E. D., Polaski, J. T., Batey, R. T., Nesbitt, D. J. J. Am. Chem. Soc. 2014, 136, 16832-16843.
Jahnke, K., Grubmuller, H., Igaev, M., Gopfrich, K. Nucleic Acids Res. 2021, 49, 4186-4195.
Jhaveri, S. D., Kirby, R., Conrad, R., Maglott, E. J., Bowser, M., Kennedy, R. T., Glick, G., Ellington, A. D. J. Am. Chem. Soc. 2000, 122, 2469-12473.
Fan, Y. Y., Li, J., Fan, L., Wen, J., Zhang, J., Zhang, Z-Q. Sens. Actuators B Chem. 2021, 346, 130561.
Kahyaoglu, L. N., Rickus, J. L. Langmuir 2018, 34, 48, 14586-14596.
Kazakov, S. A., Hecht, S. M. Nucleic acid-metal ion interactions, Encyclopedia of Inorganic Chemistry 2006, John Wiley & Sons, Ltd.
Keller, K. M.; Breeden, M. M.; Zhang, J.; Ellington, A.; Brodbelt, J. S. J. Mass. Spectrom. 2005, 40, 1327-1337.
Kemlo, J. A., Shepherd, T. M. Chem. Phys. Lett. 1977, 47, 158-162.
Li, W., Zhang, Z., Zhou, W., Liu, J. ACS Sens. 2017, 2, 663-669.
Liu, Z., Liu, B., Ding, J., Liu, J. Anal. Bioanal. Chem. 2014, 406, 6885–6902.
Lopez, A., Liu, J. Anal. Chem. 2021, 93, 3018−3025.
Ma, H., Li, W., Zhou, W., Liu, J. ChemPlusChem 2017, 82, 1224-1230.
Marchand, A., Granzhan, A., Iida, K., Tsushima, Y., Ma, Y., Nagasawa, K., Teulade-Fichou, M-P., Gabelica, V. J. Am. Chem. Soc. 2015, 137, 750−756.
Mei, M., Mu, L., Liang, S., Wang, Y., She, G., Shi, W. Biosens. Bioelectron. 2021, 178, 113025.
Merino, E. J., Weeks, K. M. J. Am. Chem. Soc. 2005, 127, 12766-12767.
Mikkelsen, N. E., Johansson, K., Virtanen, A., Kirsebom, L. A. Nat. Struct. Biol. 2001, 8, 510-514.
Ngororabanga, J.M.V., Moyo, C., Hosten, E., Mama, N., Tshentu, Z.R., Anal. Methods 2019, 11, 3857–3865.
Nutiu, R., Li, Y. J. Am. Chem. Soc. 2003, 125, 4771-4778.
Reuss, A. J, Vogel, M., Weigand, J. E., Suess, B., Wachtveitl, J. Biophys. J. 2014, 107, 2962–2971.
Rupcich, N., Chiuman, W., Nutiu, R., Mei, S., Flora, K. K., Li, Y., Brennan, J. D. J. Am. Chem. Soc. 2006, 128, 780-790.
Sissoeff, I., Grisvard, J., Guillé, E. Prog. Biophys. Molec. Biol. 1976, 31, 165-199.
Sorokin, D. A., Valeev, V. A., Gladchenko, G. O., Degtiar, M. V., Blagoi, Y. P. Macromol. Biosci. 2001, 1, 191-203.
Stojanovic, M. N., de Prada, P., Landry, D. W. J. Am. Chem. Soc. 2001, 123, 4928-493.
Tan, Z., Feagin, T. A., Heemstra, J. M. J. Am. Chem. Soc. 2016, 138, 6328-6331.
Ueno, Y. Anal. Sci. 2021, 37, 439-446.
Unruh, J. R., Gokulrangan, G., Wilson, G. S.; Johnson, C. K. Photochem. Photobiol. 2005a, 81, 682-690.
Unruh, J. R., Gokulrangan, G., Lushington, G. H., Johnson, C. K., Wilson, G. S. Biophys. J. 2005b, 88, 3455-3465.
Varnes, A. W.; Dodson, R. B.; Wehry, E. L. J. Am. Chem. Soc. 1972, 94, 946–950.
Wang, R. E., Zhang, Y., Cai, J., Cai, W., Gao, T. Curr. Med. Chem. 2011, 18, 4175-4184.
Xia, T., Yuan, J., Fang, X. J. Phys. Chem. B 2013, 117, 48, 14994-15003.
Yu, X., Wu, X., Bermejo, G. A., Brooks, B. R., Taraska, J. W. Structure 2013, 21, 9-19.
Zhang, D., Shen, H., Li, G., Zhao, B., Yu, A., Zhao, Q., Wang, H. Anal. Chem. 2012, 84, 8088−8094.
Zhao, Q., Lv, Q., Wang, H. Anal. Chem. 2014, 86, 1238-1245.

Zhou, X. H., Kong, D. M., Shen, H. X. Anal. Chem. 2010, 82, 789-793.
Zimmermann, G. R., Wick, C. L., Shields, T. P., Jenison, R. D., Pardi, A. RNA, 2000, 6, 659-667.

Figure 1. Schematic representation of the quencher metal ion-based signaling approach. In the free state of the tracer, the fluorescent intensity is diminished by the quencher binding to DNA. The formation of the target-aptamer complex could cause a decrease (i) or an increase (ii) in the binding of quenchers along the strand, leading to an analyte-dependent change in the fluorescent signal.

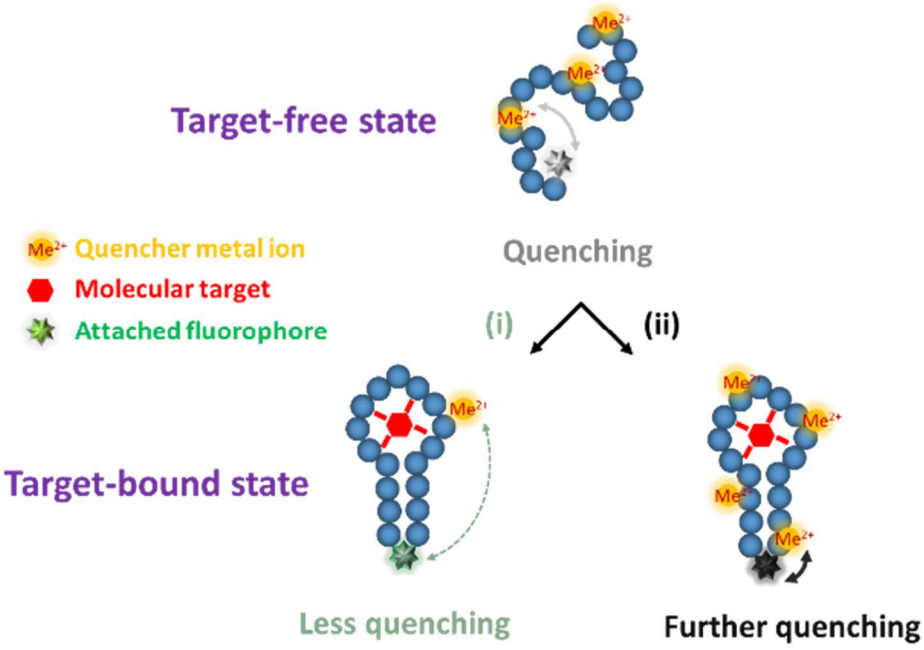

Figure 2. Effects of metal ions (400 µM) on the response of the 3'-F-apt-T and 3'-TR-apt-T probes (30 nM). 50 mM MES buffer. FI_m and FI_0 are the fluorescence intensity in the presence and absence of metal ions, respectively ((*) a nearly complete quenching was recorded for 3'F-apt-T with micromolar concentrations of Cu^{2+}, see also Figure 3). Error bars represent the standard deviation from three independent experiments.

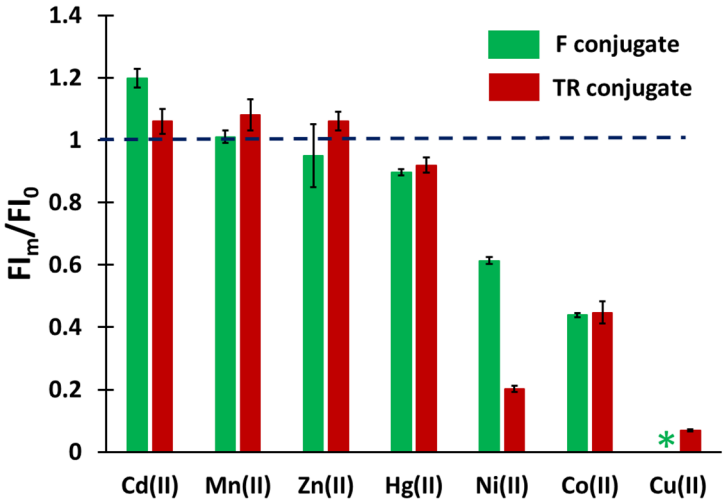

Figure 3. Metal ion titration of the 3'-F-apt-T (left) and 3'-TR-apt-T (right) probes in the absence (circle) and presence (square) of L-Tym (1 mM). 50 mM MES buffer. FI_m and FI_0 are the fluorescence intensity in the presence and absence of metal ions, respectively. Error bars represent the standard deviation from three independent experiments.

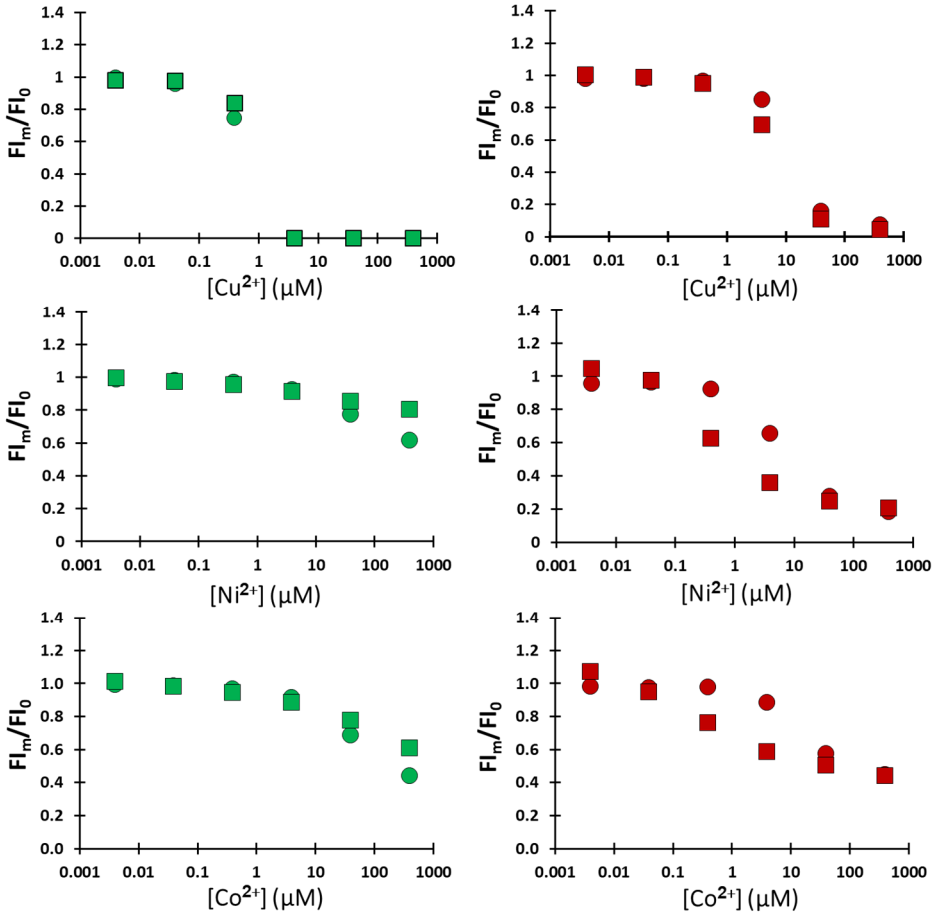

Figure 4. Dose-response curves of the 3'-TR-apt-T and control DNA probes for the L- or D-Tym analytes, in the presence of 4 μM Ni^{2+} or Co^{2+}. 50 mM MES buffer. $FI_{analyte}$ and FI_{free} are the fluorescence intensity in the presence and absence of analyte, respectively. Error bars represent the standard deviation from three independent experiments.

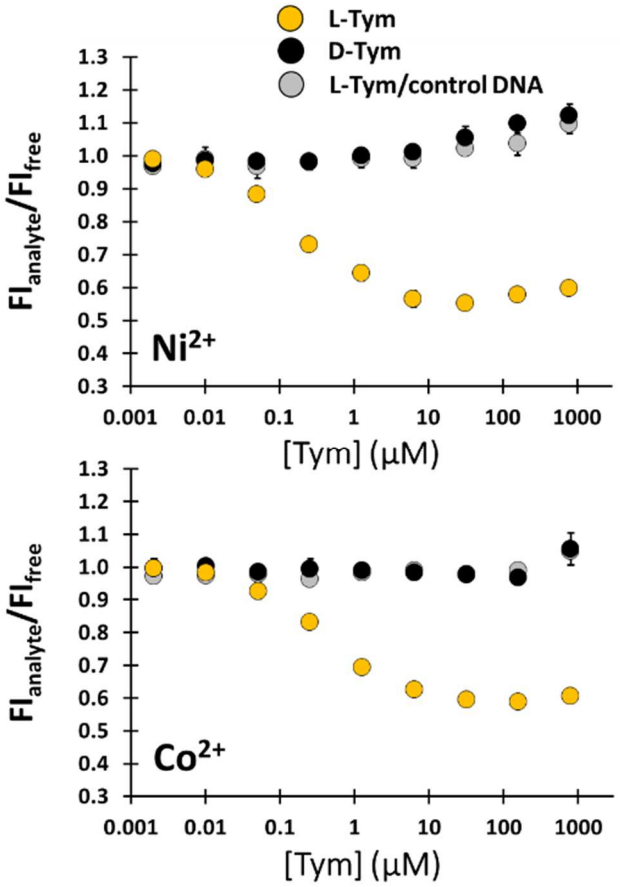

Figure 5. Metal ion titration of the 5'-F-apt-A (left) and 5'-TR-apt-A (right) probes in the absence (circle) and presence (square) of Ade (1 mM). FI_m and FI_0 are the fluorescence intensity in the presence and absence of metal ions, respectively. 50 mM MES buffer. Error bars represent the standard deviation from three independent experiments.

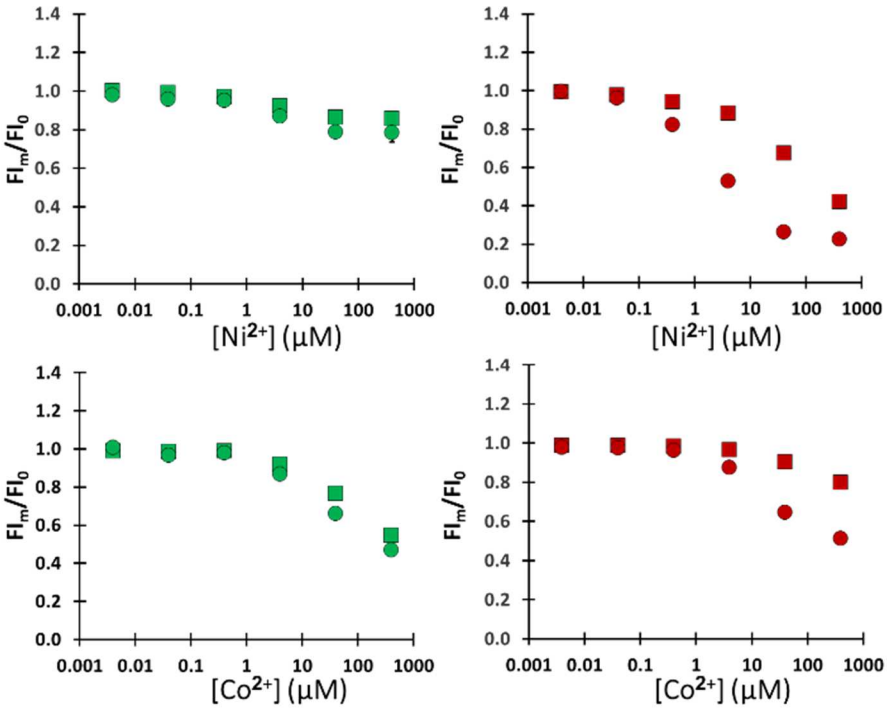

Figure 6. Dose-response curves of the 5'-TR-apt-A and control DNA probes for the Ade or Gua analytes, in the presence of 40 µM Ni^{2+} or 400 µM Co^{2+}. $FI_{analyte}$ and FI_{free} are the fluorescence intensity in the presence and absence of analyte, respectively. 50 mM MES buffer. Error bars represent the standard deviation from three independent experiments.